Journal of Achievements in Materials and Manufacturing Engineering
VOLUME 31
ISSUE 1
November
2008

Morphological and mechanical properties of hot gas welded PE, PP and PVC sheets

O. Balkan [a,*], H. Demirer [b], H. Yildirim [c]
[a] Department of Materials, Institute for Graduate Studies in Pure and Applied Science, Marmara University, Göztepe Campus, 34722, Kadikoy-Istanbul, Turkey
[b] Department of Materials, Technical Education Faculty, Marmara University, Göztepe Campus, 34722, Kadikoy-Istanbul, Turkey
[c] Department of Chemistry, Faculty of Arts and Science, Yildiz Technical University, Davutpaşa Campus, 34220, Esenler-Istanbul, Turkey
* Corresponding author: E-mail address: obalkan@marmara.edu.tr

Received 27.06.2008; published in revised form 01.11.2008

Manufacturing and processing

ABSTRACT

Purpose: The goal of the paper is to investigate morphological and mechanical properties of hot gas butt-welds on polyethylene (PE), polypropylene (PP), and polyvinyl chloride (PVC) sheets for four different procedures, which are single and double V-welds with and without a welding shoe.

Design/methodology/approach: Welding energy (E_w), which is transferred onto weld surfaces, was calculated to evaluate weld quality. Morphology of welds was analyzed by polarized light, stereo, and scanning electron microscopy.

Findings: Polarized light microscopy studies indicated that the heat-affected zone (HAZ) consists of welding rod core, molten zone, and deformed spherulitic zone. The results of tensile, bending, and impact tests indicated that the weld strengths of PVC sheets are lower than those of PE and PP sheets. When the welding shoe was used, weld strength increased significantly for each material due to the presence of sufficient welding pressure and the effective heating on surfaces.

Practical implications: The best results were attained for the double V-welds with the welding shoe.

Originality/value: Morphological and mechanical properties of hot gas welded PE, PP and PVC sheet were evaluated.

Keywords: Welding; Hot gas welding; Energy; Plastic; Polymer

1. Introduction

Hot gas welding is one of the external heating methods [19, 33, 36, 43], and it was patented by Reinhardt in 1940 [29]. In this method, a weld groove and a welding rod were heated with hot gas stream until they soften sufficiently to fuse; then, the welding rod is pressed into the weld groove. It is simple, portable, cheap, and the most suitable process in the more complex and “one-off” fabrications, and so it is widely employed to fit plastic constructions. It is used in the fabrication of chemical containers, the sealing of roof/floor membranes for coverage, and the repair of large injection molded components. However, this method has some disadvantages. The main disadvantage is that the weld quality depends on the operator skill, which is standardized by EN 13067 (European Norms). Thermal degradation and oxidation are possible because the temperature of hot gas is much higher than the melting point of the polymer being welded. Most frequently used gas is air, but the application of carbon dioxide, nitrogen, and other inert gases are mentioned. This method was detailed elsewhere [10, 12, 29-31 EN 13067;]. The method without and with a welding shoe are illustrated schematically in Fig. 1a and b, respectively. The welding shoe integrates torch and welding rod. Thus, it facilitates the welding operation as shown in Fig. 1b. This apparatus is also called as “high-speed welding nozzle”, which is widely used to heat surfaces intensively, to apply welding force sufficiently, to accelerate welding speed, and to facilitate the process for a welder [12].

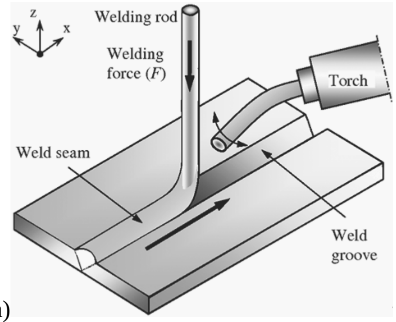

a)

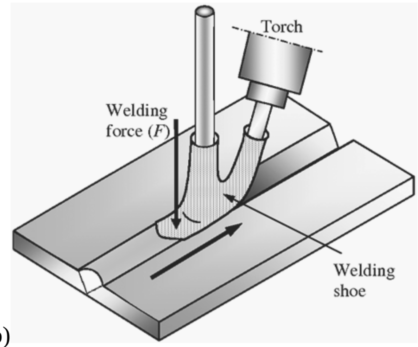

b)

Fig. 1. Schematic representations of hot gas welding (HGW); (a) Without welding shoe, (b) With welding shoe

To evaluate welding strength, weld factor, (f_w), which is also called as comparative weld strength, is expressed as

$$f_w = \frac{\sigma_{weld}}{\sigma_{base}}, \quad (1)$$

where σ_{weld} and σ_{base} are strengths of a weld and its base material, respectively. Hausdörfer et al. [13] investigated whether multilayer hot gas welding of thick polyethylene (PE) sheets (30 mm) with partially or completely plasticized welding rod can become an alternative to single-layer extrusion welding. The best results were obtained in the strength tests when hot gas and extrusion welding techniques were combined. The root layer of V-groove was welded by hot gas welding using partially plasticized welding rod, and the central and upper layers were welded by extrusion welding using fully plasticized welding materials. They attained long-term weld factors of up to 0.90 for each welding process. Diedrich and Kepme [8] studied hot gas welding of pipes and fittings made from different grades of high-density PE (HDPE). Abram et al. [1] performed hot gas welding using nitrogen gas at a temperature of 280°C on double V-grooves of unplasticized polyvinyl chloride (uPVC) and uPVC/calcium carbonate (15 wt%) sheets of 10 mm thickness. They reported that weld factors are 0.29, 0.85, and 0.94 for hot gas welded uPVC, uPVC/calcium carbonate, and hot plate welded uPVC sheets, respectively. Scanning electron microscopy (SEM) investigations showed that fracture initiates from the unfused regions in weld root for both types of materials. Obviously, the main cause for the low tensile strengths of welds was high notch sensitivity. In addition, high degree of orientation present in the welding rod may contribute to residual stress levels significantly in the welds. It was concluded that the poor thermal stability and high pseudomelt viscosity of PVC all make perfect fusion very difficult. Creep strengths of hot gas, extrusion, and hot plate welded thick PE sheets were compared by John et al. [15], who reported that weld factors are 0.57, 0.84, 0.85, and 0.98 for hot gas double V-welding, hot plate welding, extruder single V-welding, and extruder double V-welding, respectively. Hessel and Mauer [14] also studied on hot gas butt-welds for HDPE, polypropylene (PP), and PVC pipes. Atkinson and Turner [2] designed a new jig to reduce weld pores through the escape of hot gas easily from the beneath of the weld. They investigated the effects of hot air temperature and welding pressure on mechanical properties of hot gas welded polycarbonate/polyester, poly(butylene–terephthalate), and ethylene–propylene–diene monomer (EPDM) sheets of 3 mm thickness. The weld factors of single V-welds, single V-welds with heated roller, and double V-welds (X-welds) were 0.59, 0.70, and 0.63 for the polycarbonate/polyester system, 0.76, 0.89, and 0.97 for poly(butylene–terephthalate) and 0.78, 1.00, and 0.67 for EPDM, respectively. To reduce human interference on the welding parameters such as welding speed, welding force, welding temperature, and flow rate of hot gas, a hot gas welding portal was designed and built by Marczis and Czigany [19-21], who reported that the tensile strength of hot gas welded PP sheets reach 19 MPa when the welding force range was 12–16 N. The heat-affected zone (HAZ) of welds is divided into three well-distinguishable parts, namely the cool, plastic, and flow zone of the weld center [21]. Cramer [7] explained and classified weld defects for hot gas, extrusion, and hot plate welding as undercuts in the base material and on the root, incomplete and excessive fusion, pores, reinforcement on welds, etc. Pollutants from laser cutting and hot gas welding of PP, PVC, PC, PMMA, and PA6 sheets were studied by Sims et al. [35], who performed hot gas welding for 4 h in a cabinet and obtained a simple mixture of substances in small quantities with no detectable particulate content.

The aim of this work is to investigate the effects of widely used welding procedures, which are single and double V-welds with and without welding shoe, on weld morphology and weld strength of hot gas welded PE, PP, and PVC sheets. In addition, to evaluate the weld quality, welding energies were calculated by considering welding parameters, such as welding temperature, welding speed, and flow rate of gas. Microstructures of welds as well as weld defects were investigated by polarized light microscopy Fracture surfaces were examined by stereomicroscopy and SEM to observe defects in the welds. Tensile, bending and Izod impact tests were performed to analyze mechanical properties.

2. Experimental

2.1. Materials and equipment

The hot gas welding was performed on 3 mm thick extruded sheets of polyethylene (PE-HWST 235741), polypropylene (PP-

DWU 534721), and polyvinyl chloride (PVC-CAW 311541), manufactured by SIMONA® AG (Kirn, Germany). Extruded welding rods having a diameter of 3 mm were made of the same materials (EN 12943), also by SIMONA AG. Technical data of each material is given in Table 1 (SIMONA catalogue). Welding operations were carried out using a LEISTER® 1G1 TRIAC PID model hot air welding machine (Electro-Getabeau, Kagiswil, Switzerland) equipped with the welding shoe (no. 27). This welding machine has a constant airflow capacity of 230 L min^{-1} (38.33×10^{-4} m^3 s^{-1}). The temperature of air is electronically adjustable between 20 and 700°C (LEISTER hot air gas welding machine user's guide).

2.2. Hot gas welding process

The hot gas welding was performed according to EN 13067. The sheet edges were cut to produce 60° single V-grooves and double V-grooves (X-grooves) as shown in Fig. 2a and b, respectively.

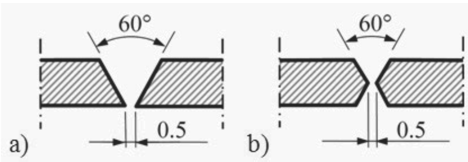

Fig. 2. Geometries of weld grooves (y–z plane). (a) Single V-weld groove. (b) Double V-weld groove

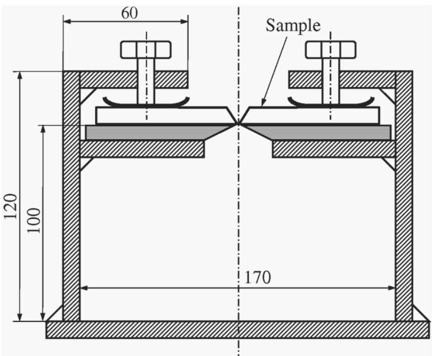

Fig. 3. A cross-sectional view of the welding jig

The weld specimens were then fixed in a suitable jig (Fig. 3) to minimize thermal distortions and porosity in the welding zone [2]. The weld groove and the welding rod were then heated to fuse by the hot gas welding machine (welding torch), as shown in Fig. 1a and b. Welding temperatures are usually above glass transition temperatures for amorphous polymers or above melting temperatures for semi-crystalline polymers to mobilize polymer chains at interface through reductions in viscosities of molten polymers. In order to accelerate welding speed, high temperatures of hot gas were preferred as far as possible. The optimum air temperature for each material was determined by means of welding trials and manufacturer's suggestions (SIMONA catalogue). The determined temperatures were 320°C, 305°C, and 365°C for PE, PP, and PVC, respectively. During the examinations of preliminary welds, it was found that insufficient fusion might take place on the surfaces of the work pieces below the determined temperatures. On the other hand, above these temperatures, welding region was deformed as well as burned partially when the material was PVC. In addition, the best results were attained when the gap of groove root was 0.5 mm. The welding force (F_w) applied on the welds was in the range of 10–20 N (welding pressure: 1.4–2.8 MPa) when the welding shoe was employed. However, it was ~5 N (welding pressure: ~0.7 MPa) without the welding shoe owing to bending of the welding rods during welding operations. The welding shoe on the nozzle of the torch maintains the welding pressure on the partially molten rod and ensures penetration into the weld groove.

2.3. Test methods

For polarized light microscopy studies, thin slices (10 μm) were cut from the welded specimens into y–z plane using a Leica R6125 model rotary type microtome. These thin slices were investigated using a Leica DMLP model polarized light microscope. Fig. 4 shows preparation of test specimens. Morphological features as well as some weld defects could be observed when polarized light is used. An Olympus SZ60 model stereomicroscope was also used to visualize 3D-fracture surfaces of welds (EN 13100-1). For SEM analysis, fractured surfaces (x–z plane) of welded specimens were coated with gold and examined with a JEOL JSM-5910LV model SEM at 10 kV.

Bending and tensile tests were carried out according to EN 12814-1 and -2, respectively, using an Instron 1011 model universal testing machine at a strain rate ($\dot{\varepsilon}$) of 33.3×10^{-4} s^{-1}. Izod impact tests were performed according to EN ISO 180 using an IM. 01 model impact testing machine on $10 \times 3 \times 63.5$ mm^3 rectangular strips. Impact test was applied onto both top and bottom sides of specimens separately (onto x–y plane) to determine impact strengths of the weld face and the weld root for the single V-welds and those of the first and the second seams for the double V-welds. Bending tests were performed also on both sides of specimens separately.

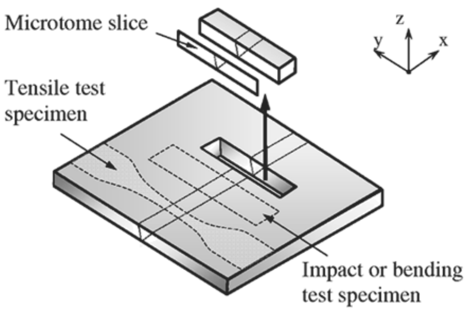

Fig. 4. Preparation of test specimens

Table 1.
Properties of PE, PP, and PVC sheets (SIMONA catalogue)

Materials	σ_y (MPa)	ε_y (%)	E-Modulus (GPa)	Notched impact strength (kJ m^{-2})	Hardness (Shore D)	Thermal coefficient of elongation (K^{-1} ×10^{-4})	Thermal conductivity (W m^{-1} K^{-1})
PE	22	9	0.8	13	62	1.8	0.38
PP	32	8	1.4	7	72	1.6	0.22
PVC	58	4	3.0	4	82	0.8	0.16

Table 2.
Welding speeds (S_w) and welding energies (E_w) of PE, PP and PVC welds

Welding procedures	PE		PP		PVC	
	S_w (mm s^{-1})	E_w (kJ m^{-1})	S_w (mm s^{-1})	E_w (kJ m^{-1})	S_w (mm s^{-1})	E_w (kJ m^{-1})
V-weld	1.3	1074.3	1.0	1326.7	3.0	535.3
X-weld	1.5[a] (0.8)	1862.1[b]	1.2[a] (0.6)	2211.2[b]	3.8[a] (1.9)	845.3[b]
V-weld with welding shoe	5.0	279.3	4.5	294.8	6.7	239.7
X-weld with welding shoe	5.5[a] (2.8)	507.8[b]	4.8[a] (2.4)	552.8[b]	7.1[a] (3.6)	452.4[b]

[a] Welding speed (S_w) were measured on one of the two seams. The true welding speed values of double V-welds (X-welds), which are shown in parentheses, are half since a double V-weld comprises two seams; [b] Welding energy (E_w) were calculated using the true welding speeds of corresponding double V-welds.

3. Results and discussions

3.1. Welding energy (E_w)

To achieve good quality welds, it is necessary to determine the effects of the welding parameters and their interrelations on the welds. Good quality welds can be obtained when adequate amount of energy is transferred onto the weld surfaces. In the case of hot gas welding method, this energy is taken to the surfaces in a blowing gaseous medium. The energy can be determined when the gas is streaming through the welding machine. Thermodynamic and gas dynamic aspects can be helpful in the evaluation of weld strength. For the hot gas welding method, the welding energy (E_w) can be calculated as

$$E_w = \frac{c_p (T_2 - T_1) q_v \rho}{S_w}, \qquad (2)$$

where E_w is welding energy, c_p is specific heat of the gas, T_1 and T_2 are entering and leaving temperatures of the flowing gas, q_v is volume flow rate of the gas, ρ is density of the gas, and S_w is the welding speed [20, 21]. Apart from the necessary conditions for good welds, i.e. largest common surface, similar surface energies, compatibility, similar thermal contractions, the parameters related to welding energy are temperature, deformation kinetics, and crystallization kinetics. These parameters influence crystallization of weld and, therefore, weld strength of crystalline polymers. Bonten and Schmachtenberg [5] proposed that mixed recrystallization of the molecular chains of both components in the weld is possible, and it increases weld strength after a short time. During the welding process, heating time and temperature can influence crystallization kinetics and the building of interlaminar links, and the flow rate of the melt influences the deformation kinetics.

The welding speeds for each welding procedure and material were measured during the welding operations, and their welding energies were calculated using *Eq.* 2. Values of welding speed and welding energy are given in Table 2. When the welding shoe was used, welding speeds increased about 4, 5, and 2 times more for PE, PP, and PVC, respectively. For double V-welding, the welding speed was measured on one of the two seams. The speeds of double V-welding were found to be higher than the speeds of single V-welding, since the size of the double V-weld groove is smaller than the size of the single V-weld groove. However, the true welding speed of a double V-weld is equal to half of the measured welding speed because a double V-weld comprises two seams. Therefore, the welding energy of a double V-weld is calculated using the true welding speed. In addition, the welding energy of a weld with and without the welding shoe is not comparable due to heat intensification effect of the welding shoe on the welding process.

The welding energies of double V-welds were found to be higher than single V-welds for all three types of thermoplastics. For each welding procedure, the welding energies of PVC were lower than those of PE and PP as shown in Table 2, because of sensitivity of PVC to thermal degradation. High welding energy values reduce viscosity of the material on the welding surfaces leading to increase in weld strength through diffusion. Marczis and Czigany [20, 21] reported that the weld strength of single V-welded PP sheets with the welding shoe increase with increasing welding energy. They also found that the weld strength reached a maximum value of 19 MPa when the welding energy varied in the range of 0.37–0.46 kJ mm^{-1} with a welding force of 10–12 N.

3.2. Morphology

A region in which the structure is affected by the applied heat is defined as the HAZ. Based on the polarized light micrographs, typical y-z cross sections of single and double V-welds are drawn schematically as shown in Fig. 5a and b, respectively. It was found that the HAZ consists of three main zones, namely welding rod core, molten zone, and deformed spherulitic zone for PE and PP welds. Polarized light micrographs of welding cross sections for PE, PP, and PVC welds are shown in Figs. 6-8, respectively.

The zone of welding rod core forms, since the welding rod is not molten completely. Sacks [31] and Gumbleton [10] mentioned that the outer surface of the rod is molten while the inner core remains merely flexible during welding operation. Hausdörfer [13] proposed that the welding rod is not molten completely during welding process; therefore, the welder has to exert too much force in deforming welding rod, especially thick ones.

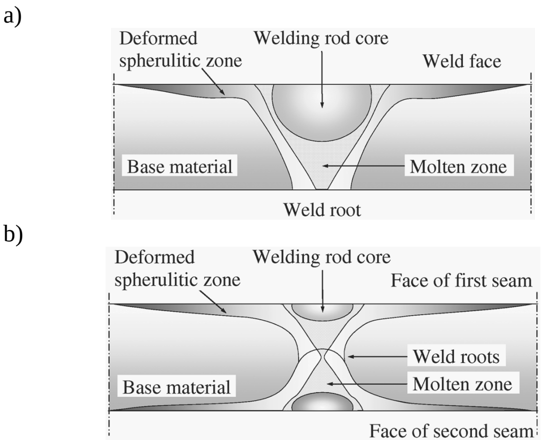

Fig. 5. Schematic representations of the heat affected zone (HAZ) in the welding cross section (y–z plane); (a) Single V-weld, and (b) double V-weld

Deformed spherulitic zone was broadened significantly when welding was performed without the welding shoe. Thermal distortions as well as deformed spherulitic zone were reduced when the welding shoe was used, since the hot gas is restricted to a narrow region. It was found that the boundaries of the HAZ appear more clearly than the interface as shown in Fig. 6a and b for welded PE and Fig. 7a and d–g for welded PP sheets. As can be seen from Fig. 6c for welded PE and Fig. 7b and e for welded PP sheets, interface was distinguishable from the bulk materials when the welding was performed without the welding shoe. On the other hand, interface was indistinguishable from bulk materials due to the application of sufficient welding pressure and intensive heating shown in Fig. 7c and d. In this case, a group of coarse spherulites was developed typically in place of the interface. This result can be attributed to the effect of slow cooling rate as shown in Fig. 7c. Streamlines were observed at the boundaries of molten zone. These streamlines are in fact incompletely molten and sheared layers, which were the result of the combined effect of rapid cooling and shear stresses.

The molten zone must not be necessarily large in volume but must exist in order for the polymer chains to fuse across the interface. Michel [23, 24] developed a mathematical model for the heating phase of extrusion welding and showed that weld quality is affected by heating phase and molten layer thickness in the base material. For extrusion V-welded HDPE sheets, high creep strength was attained at a molten layer thickness of about 0.25 mm. Potente et al. [28] obtained a small HAZ region for laser transmission welding of HDPE. Becker and Potente [4] also showed that laser transmission welded PP containing 0.1 wt% of carbon black attains a molten layer thickness up to 1.25 mm.

Marczis and Czigany [20] reported that the HAZ of hot gas butt V-welded PP sheets have three well distinguishable regions, namely the cool, plastic, and flow zone of the weld center. From base material to weld centre, the following supermolecular structures were observed, coarse spherulites of base material, streamline formation in the sheared melt, a fine spherulitic structure and spherulites whose size gradually increases when moving toward the weld centre. They proposed that the weld strength increases with increasing width of the HAZ. The width of the HAZ decreased with decreasing welding energy and with increasing welding force, and it reached a maximum of 0.4 mm with a welding energy up to about 0.38 kJ mm^{-1} at a welding force of 15 N. They also reported that weld strength increases with the decreasing ratio of weld width to weld height. Some researchers [1, 2] noted that the removal of surface irregularities by weld dressing do not change the weld strength significantly. Therefore, the unfused regions within the joints are more important than surface defects.

Schmachtenberg and Tüchert [32] reported that the HAZ of hot plate welded PP sheets can be divided into well-distinguishable six regions that are taken perpendicular to the weld axis from the centreline of the weld to the base material. In the centreline of the seam, a transcrystalline structure made up of linear spherulites, in the next, coarse spherulitic zone similar to that of the base material were observed. It is followed by a thin, fine spherulitic layer formed due to rapid cooling. The streamlines in the sheared molten zone were the results of the combined effects of rapid cooling and shear stresses. Increases in the welding temperature increased the width of the sheared molten zone, but the width of the fine spherulitic layer was independent of the welding parameters. In the incompletely molten and sheared zone, the spherulites were only partially molten compared to the sheared molten zone. Finally, the base material did not melt at all and coarse spherulites could be observed in it.

Gehde and Ehrenstein [9] revealed that bending strength of extrusion V-welded thick PP sheets (10–20 mm) attains a maximum value when molten layer thickness is in the range of 0.5–0.8 mm. They found a multilayer structure that consists of deformed spherulite layer, recrystallized layer and transcrystalline layer, starting from base material to weld center. Shape of the molten layer is a function of the hot air temperature, the welding speed, geometry of the air nozzle, and thickness of the work parts. V-shaped hot air nozzle is designed to produce thin and uniform molten layer. The tubular-shaped nozzle produced a very thick molten layer, but the thickness changed along the joining surface. Oliveira [26] mentioned that the weld quality is affected by the key morphological factors. The occurrence of these morphological features and defects in the weld seams depend on welding parameters. Crystal structure formation in the HAZ of hot plate welded PP sheets were also investigated by Nieh and Lee [25], who observed at least three different crystallization structures around the joint interface i.e. stressless recrystallization region, the columnar region, and slightly deformed region, starting from weld center to base material. In recrystallization region, viscosity and modulus of the molten polymer are smaller owing to the high temperature. Therefore, the material in this region has a lower stress level and a longer time for stress relaxation and recrystallization. In the columnar region, elongated spherulites oriented along the flow direction. The deformed crystals indicated that crystallization takes place under shear stress. This structure is called as stress-induced crystal structure. In this region, viscosity and modulus are high owing to the lower temperature. Consequently, the crystals are formed under the influence of flow stress.

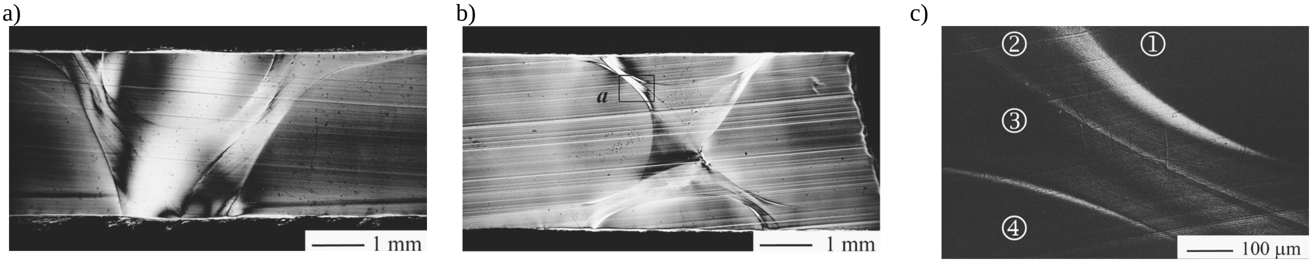

Fig. 6. Polarized light microscopy micrographs of welded PE sheets. (a) Single V-weld. (b) Double V-weld. (c) Magnified view of frame *a* in (b); (1) core of welding rod; (2) molten zone; (3) deformed spherulitic zone, and (4) base material

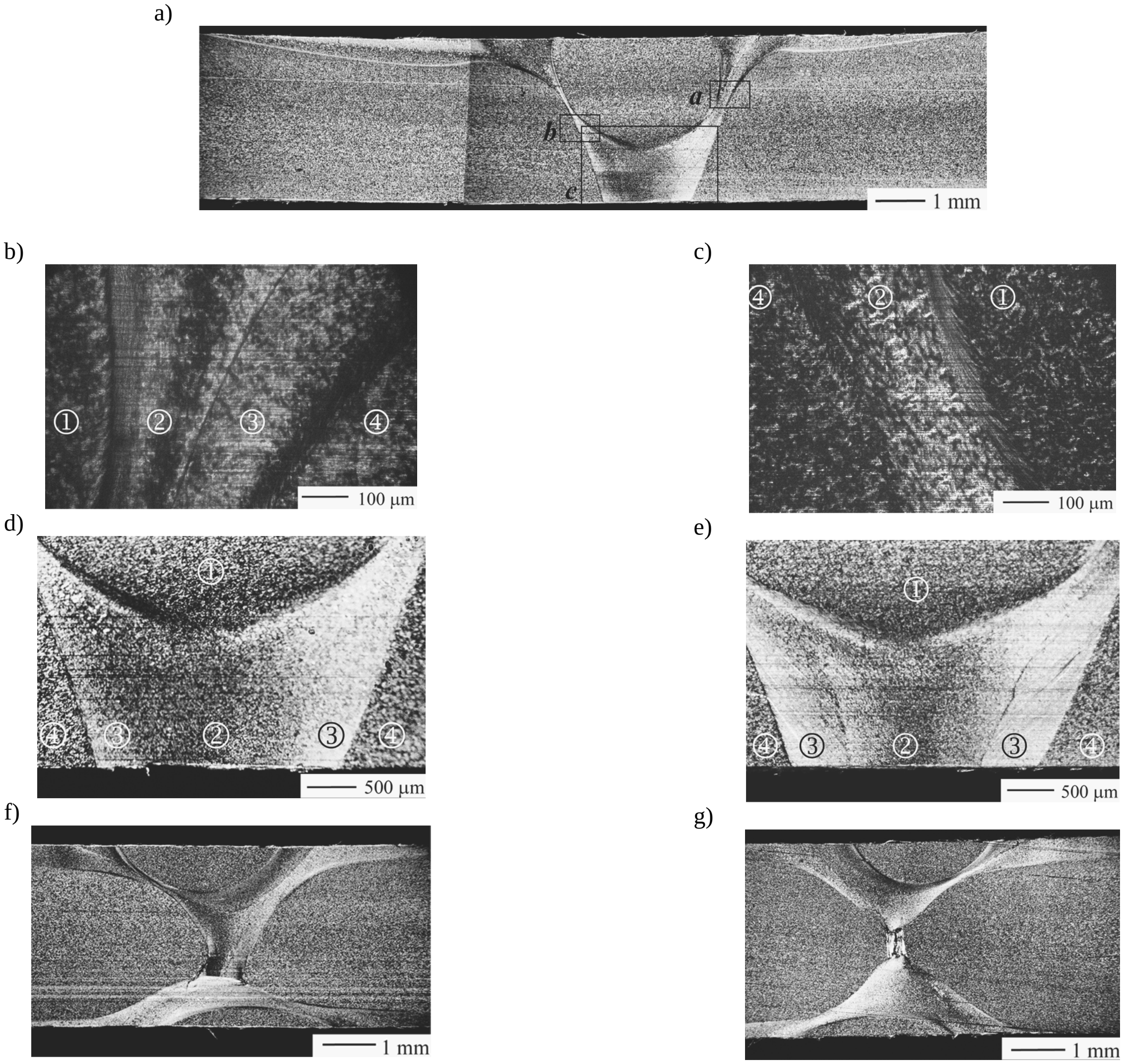

Fig. 7. Polarized light microscopy micrographs of welded PP sheets. (a) Single V-weld. (b) Magnified view of frame *a* in (a). (c) Frame *b* in (a). (d) and (e) frame *c* in (a) with and without welding shoe, respectively. (f) and (g) double V-welds with and without welding shoe, respectively. For the numbers on the micrographs see Fig. 6

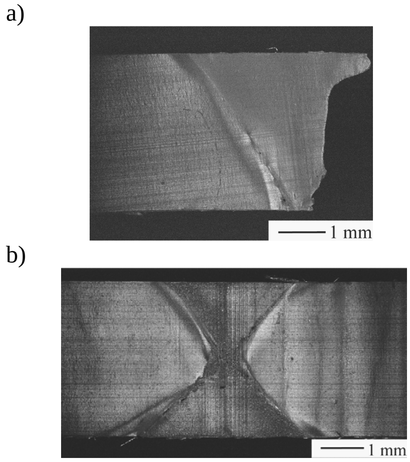

Fig. 8. Polarized light microscopy micrographs of welded PVC sheets. (a) Single V-weld. (b) Double V-weld

Typical weld defects can be detected by polarized light microscopy. Unfused interfaces are shown in Fig. 6a-c for PE, Fig. 7b, e and g for PP welds, Fig. 8a, b for PVC. Internal cracks in weld root are shown in Fig. 7f for a PP weld. Unfused root of a weld, which was performed without the welding shoe is given in Fig. 7g for a PP weld. Discontinuities at the interface are shown in Fig. 8a and b for PVC welds. It was found that insufficient fusion takes place when the welding shoe is not used, as shown in Fig. 7e and g for PP welds. It should be noted that weld face of all three materials contains less defect than weld roots, inferring higher weldability (rheological weldability, RW) of weld face due to high temperature, high shear rate and low viscosity of weld face [3]. Weldabilities of these thermoplastics were assessed through their rheological properties and activation energies by Balkan et al.[3].

The zones were clearly observed for PE and PP welds because of their semicrystalline structure, while the zones disappeared for PVC due to its amorphous structure. However, Lin and Wu [17] observed three main regions which are plasticized region, partly plasticized region, and undeformed region on polished weld cross sections of spin-welded PVC. It was observed that the interface in PVC welds contains discontinuities and defects. This may be due to the presence of partially burned PVC which formed during welding. Stokes [38] observed that molten surfaces of PVC could be oxidized during hot plate welding when these surfaces were exposed to air.

In this study, only fractured surfaces (x–z plane) of welded PP and PVC sheets were analyzed by stereomicroscopy and SEM, because the welded PP and PVC sheets were broken during Izod impact test, while welded PE sheets were not. However, y–z plane of welded PE sheets, which were broken during tensile tests, were valuable for examination. Figure 9a and b show weld areas for single and double V-welded PE sheets, respectively. Their weld faces were strained by tensile stress, while the weld roots were not, because weld roots of single and double V-welded PE sheets are brittle. Failure occurred first at the weld root, the weakest point of the welding region. Unfused regions in the weld roots were detectable when fractured surfaces of single and double V-welded PP and PVC sheets were analyzed by stereomicroscope as shown in Figs. 10 and 11, respectively.

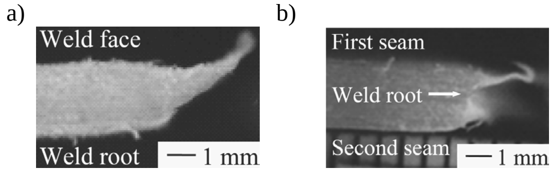

Fig. 9. Stereomicrographs of welded (tensile tested) PE sheets (y–z plane). (a) Single V-weld. (b) Double V-weld

SEM micrographs were selected to illustrate the principal defects that occur in the hot gas welding. Unfused regions were found at the boundaries between the weld and base materials in weld root. Figure 12a shows an unfused region and pores in weld root of a single V-welded PP sheet. The pores form due to the closed weld root gap. Therefore, hot gas cannot escape from the beneath of the weld. Unfused regions in the weld root were typical for double V-welded PP and PVC sheets. One can say that the first seam more compatible with base material than the second seam for double V-welded PP sheets as shown in Fig. 12b. When welds for PP and PVC were compared, it was found that welding compatibility of PP is higher than that of PVC as shown in Figs. 12b and 13 for PP and PVC welds, respectively.

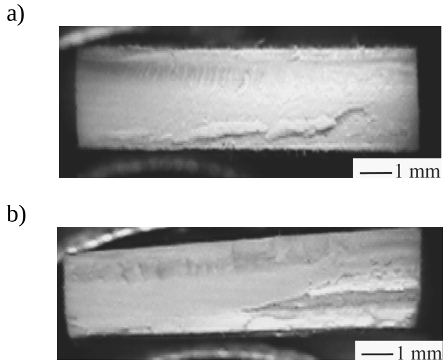

Fig. 10. Stereomicrographs of welded and fractured PP sheets (x–z plane). (a) Single V-weld. (b) Double V-weld

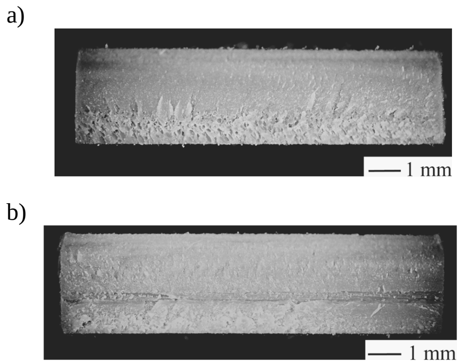

Fig. 11. Stereomicrographs of welded and fractured PVC sheets (x–z plane). (a) Single V-weld. (b) Double V-weld

a)

b)

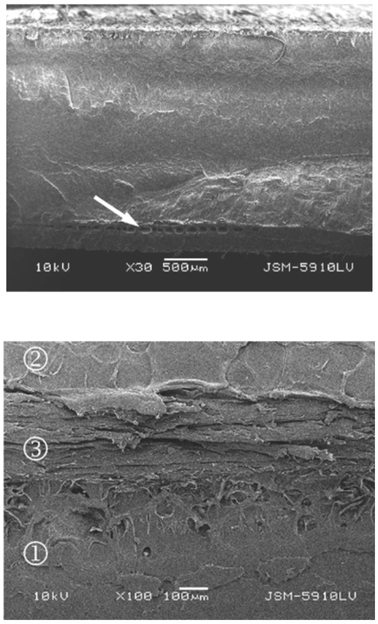

Fig. 12. SEM micrographs of welded and fractured PP sheets (x–z plane). (a) Single V-weld; the arrow shows pores in the weld root. (b) Double V-weld; (1) the first seam; (2) the second seam; (3) unfused region in weld root

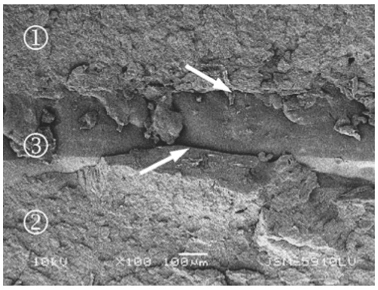

Fig. 13. A SEM micrograph of double V-welded and fractured PVC sheet (x–z plane); the arrows show fracture initiation line in the weld root. For the numbers on the micrographs see Fig. 12

3.3. Mechanical properties

In the present study, the welded specimens always fractured at welds with low elongations. Stress and strain at yield of welded specimens were found to be lower than their base ones as shown in Fig. 14. Two common theories were proposed on why weld strength is weaker than base material [32]. One theory is "structural change theory" which involves the locally diversified structure within the weld, i.e. the crystallization condition strongly depends on the thermal history. The other theory is "aging theory" which involves the actions of heat and oxygen that cause a thermo-oxidative decomposition of polymer molecules.

Tensile, impact, and bending test results of all three types of thermoplastic sheets are given in Table 3. Weld factors varied in the range of 0.77–0.90 and 0.63–0.80 for PE and PP, respectively, while it varied in the range of 0.45–0.77 for PVC. From the values of the weld factors, it can be said that the weld strength of PVC is the lowest. Marczis and Czigany [19] mentioned that the semi-crystalline materials such as PE and PP can easily be welded, while amorphous ones, such as PVC, exhibits difficulty in welding. The reason for this difficulty is the slow melt flow followed by quick degradation. Yield strains of the welded specimens varied nearly parallel to the weld factors as shown in Table 3. Weld factors increased significantly when the welding shoe was used for both single and double V-welds. In fact, for double V-welds with the welding shoe, the calculated weld factors attained the maximum values which were 0.90, 0.80, and 0.77 for PE, PP, and PVC, respectively. Strength of double V-welds is expected to be higher than single V-welds since double V-welds have higher welding energy and effective welding pressure.

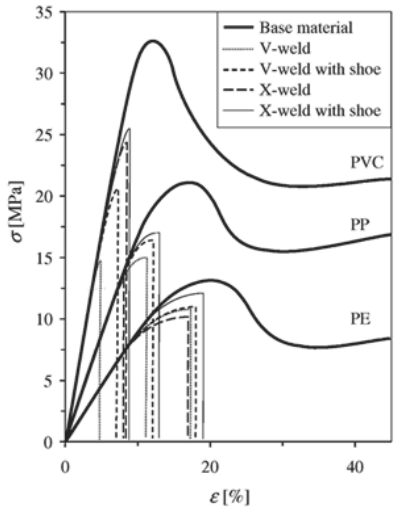

Fig. 14. Stress–strain (σ–ε) curves for base and welded PE, PP, and PVC sheets with various welding procedures

Haim [11] mentioned that double V-welds are stronger than single V-welds but they are also more tiresome to make. In general, double V-welds 10–20% stronger than any of other type of welds in rigid PVC. However, in the present study, weld factors of double V-welds on PE and PP sheets were found to be lower than their single V-welds when the welding shoe was not used. The reason for this is that the second seams of the double V-welds may have contained some discontinuities. The second grooves were likely being exposed to oxidation during welding process of the first seams. Schmachtenberg and Tüchert [32] reported that the weld strength is reduced by a high consumption of antioxidants and thermo-oxidative decompositions of polymer molecules during welding. Apart from the oxidation, pores may take place in the second seam since its root is closed by the first seam. Atkinson and Turner [2] reported that pores in a weld are reduced when the root of weld groove is open.

Welds of PP and PVC fractured during Izod impact tests while base specimens of all three types of materials and welded PE specimens were not. Welded PVC sheet absorbed the lowest

Table 3.
Mechanical properties of welded PE, PP, and PVC sheets with standard deviations, which are shown in parentheses in italic form

	f_w (-)	σ_y (MPa)	ε_y (%)	Izod impact strength (kJ m^{-2})		Break angle (°)	
				a	*b*	*c*	*d*
PE							
Base material		13.22 *(0.24)*	20.40 *(0.82)*	NB	NB	NB	NB
V-weld	0.82	10.78 *(0.34)*	17.12 *(1.10)*	NB	NB	70 *(2.12)*	63 *(1.58)*
X-weld	0.77	10.13 *(0.62)*	17.07 *(1.16)*	NB	NB	75 *(1.41)*	67 *(2.12)*
V-weld with welding shoe	0.84	11.12 *(0.26)*	17.84 *(1.22)*	NB	NB	74 *(2.24)*	69 *(1.41)*
X-weld with welding shoe	0.90	11.91 *(0.18)*	19.04 *(0.59)*	NB	NB	86 *(1.00)*	84 *(1.22)*
PP							
Base material		21.12 *(0.51)*	17.28 *(0.43)*	NB	NB	NB	NB
V-weld	0.71	15.02 *(0.88)*	11.33 *(1.07)*	17.11 *(1.01)*	14.06 *(1.08)*	51 *(1.87)*	39 *(1.22)*
X-weld	0.63	13.33 *(0.95)*	08.11 *(0.92)*	24.37 *(0.92)*	17.74 *(1.21)*	64 *(2.24)*	52 *(2.12)*
V-weld with welding shoe	0.77	16.19 *(0.93)*	11.96 *(0.46)*	24.09 *(1.11)*	22.93 *(1.21)*	63 *(2.35)*	56 *(2.35)*
X-weld with welding shoe	0.80	16.88 *(0.39)*	12.94 *(0.43)*	35.27 *(0.42)*	29.24 *(0.86)*	75 *(0.71)*	69 *(1.00)*
PVC							
Base material		32.62 *(0.36)*	12.24 *(0.22)*	NB	NB	NB	NB
V-weld	0.45	14.82 *(0.85)*	04.72 *(0.87)*	08.55 *(0.91)*	05.29 *(1.28)*	29 *(1.87)*	16 *(2.35)*
X-weld	0.74	24.27 *(0.47)*	08.48 *(0.33)*	15.80 *(0.83)*	13.48 *(0.99)*	36 *(2.24)*	30 *(2.45)*
V-weld with welding shoe	0.64	20.98 *(0.76)*	07.44 *(0.54)*	15.11 *(1.21)*	13.82 *(0.88)*	34 *(2.00)*	30 *(2.00)*
X-weld with welding shoe	0.77	25.22 *(0.38)*	08.72 *(0.41)*	23.61 *(0.73)*	22.07 *(0.85)*	51 *(1.00)*	46 *(1.00)*

a, impact was on the face of single V-welds or on the first seam of double V-welds (X-welds); *b*, impact was on the root of single V-welds or on the second seam of double V-welds (X-welds); *c*, the welding face was strained for single V-welds or the first seam was strained for double V-welds (X-welds); *d*, the welding root was strained for single V-welds or the second seam was strained for double V-welds (X-welds). NB, non-break.

impact energy. As shown in Table 3, impact strengths of both single and double V-welds on PP and PVC sheets were improved significantly by using the welding shoe. Izod impact tests showed that the weld roots absorb less impact energy than the weld face for single V-welded PP and PVC sheets. This was likely the result of some weaknesses such as pores and unfused regions because of lower welding pressure on the weld root. In addition, weldability (RW) of the weld face might be better than the weld root because shear rate and temperature of the weld face are higher than those of the weld root [3]. When impacts were performed on the first seam for double V-welded PP and PVC with the welding shoe, the impact strengths attained highest values, 35.0 kJ m^{-2} and 23.6 kJ m^{-2}, respectively. The results clearly indicated the weakness of the second seams.

The welds on PE sheets broken at the highest bending angles while the welds on PVC sheets broken at the lowest bending angles. Bending angles increased significantly when the welding shoe was used for both single and double V-welds for all three types of materials. Like impact tests, bending force was applied on both sides of welds separately. When bending force applied on a surface, opposite surface was strained. Welded specimens broken at highest bending angles when the weld face of single V-welds and the weld face of the first seam of double V-welds were strained.

Results of both Izod impact and bending tests indicated the presence of weaknesses such as pores, unfused regions, and other discontinuities in the weld root. Porosity arises in a weld due to bubbles of hot gas which is trapped by a filler rod at the joint interface. Porosity in a weld can be reduced considerably when the gap of the weld root is 0.5 mm. A suitable jig can also reduce the level of porosity (Fig. 3) [2]. A further complication is unfused regions in the weld root. Unfused regions tend to act as a notch and reduce the weld strength, especially for notch-sensitive materials such as PVC [22]. Insufficient welding pressure on the weld root leads to unfused regions. Besides the flow of a molten polymer to the weld root in a short time is difficult owing to the high viscosity of polymer melts. Therefore, the diffusion of a molten polymer into the weld root is of insufficient to avoid unfused regions [10]. Since the viscosity of PVC is relatively higher than those of PE and PP, the weld root of PVC may contain unfused regions which reduce the mechanical properties of welded PVC sheets. Typical welding pressure profiles across the single and the double V-welds are demonstrated in Fig. 15a and b, respectively. The double V-welding method can overcome the unfused regions problem through exerting the pressure on both sides of the weld. Double V-welds are widely used especially for thicker cross sections. The basic design principle in built welding is that the existing cross-section must be completely connected together.

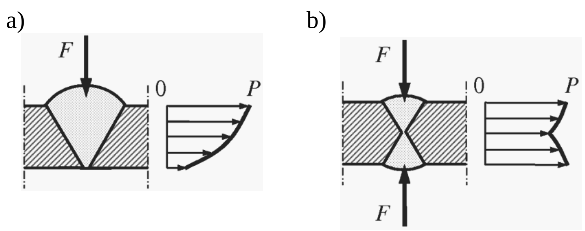

Fig. 15. Schematic representations of welding pressure (P) profiles across y–z cross section of welds. (a) Single V-weld and (b) double V-weld

In a weld, exerting pressure on the molten material helps ensure thorough mixing of the material across the interface. Insufficient welding pressure leads to reduce wettability at the interface [41]. Wool and O'Connor [40,41] proposed that weld pressure is necessary for wetting; on the other hand, inter-diffusion is retarded by increased hydrostatic pressure (more than 100 MPa) because of reduction in the volume available for the "hopping" process of segmental motion. This effect is important in polymer processing where extreme hydrostatic pressure are encountered but is not very important in normal tack experiments such as welding, where the contact pressures are less than 100 MPa. In the present study, a welding pressure of maximum 3 MPa was applied. Atkinson and Turner [2] insisted on the necessity to apply sufficient pressure on a hot gas weld to obtain satisfactory weld strength, and reported that weld strength and interfacial bonding improve if a heated roller is used immediately following the welding torch to compress the molten polymer. Michel [23] mentioned the importance of extrusion V-welds on HDPE. Good quality welds can be obtained when the welding pressure is set in such a way that full root fusion is guaranteed. In the present work, defect-free welds obtained when the welding shoe was used to compress the hot welding material.

Diedrich and Kempe [8] studied hot gas welding of pipes and fittings made from different grades of HDPE. They reported that long-term weld factors for creeps test are 0.35 (up to 0.60), 0.60, and 0.90 for hot gas single V-welds, extrusion V-welds, and hot plate welds, respectively. Hessel and Mauer [14] also studied hot gas butt welds made of HDPE, PP, and PVC and reported that specimens, which fractured at higher bending angles, have larger ductile zone which exhibits scalloped stretching area on their fracture surfaces. Kolbasuk [16] reported that strength of hot wedge fusion welded HDPE geomembranes is equal to the yield strength of their base material. Shoh [34] reported weld factors of ultrasonic welds on PE, PP, and PVC in the range of 0.90–1.00, 0.90–1.00, and 0.40–1.00, respectively. Wu and Benatar [42] reported weld factors for microwave welds on HDPE composites as high as 0.96. Staicovici et al. [37] also found weld factors for microwave welds on HDPE in the range of 0.85–0.95. Bowman [6] reported a weld factor for hot plate welds on PE as high as 0.61. Potente et al. [28] obtained weld factors of laser welds on PE/carbon black composites in the range of 0.60–1.00. Schmachtenberg and Tüchert [32] studied hot plate welded PP sheets and reported a weld factor about 0.90 and bend angle in the range from 9° to 12° at a testing temperature of 230°C. Lin et al. [18] reported a weld factor for non-contact hot plate welds on PP as high as 1.00. Oliveira et al. [26, 27] investigated hot plate welded PP filled with 20 and 30% of talc, the latter flame retarded grade, and reported that the maximum weld factors are 0.50 and 0.45, respectively. Stokes [38] assessed weldability of two grades of PVC, having tensile strengths of 57.7 MPa and 63.2 MPa, through hot plate and vibration welding, and reported that their weld factors for both welding methods are about 0.85 and 0.97 with corresponding failure strains of about 2.5% and 3.3%. He [39] also reported a weld factor for induction welded PP as high as 0.55. According to some researchers [8, 13, 32], long-term tests such as creep test were more adequate than short-term tests in the determination of weld strength, because the long-term behavior of welds reveals more specific differentiation of weld strength.

4. Conclusions

Values of welding energy (E_w) input into PE and PP welds were found to be higher than that of PVC. This indicated that PVC is more sensitive to thermal degradation than PE and PP. It was also showed that double V-welds contain higher values of welding energy than single V-welds. This means that strength of double V-welds can be higher than single V-welds.

Based on the polarized light microscopy studies, the HAZ consists of three main zones, namely welding rod core, molten zone, and deformed spherulitic zone for PE and PP. Interface was indistinguishable from bulk materials when welding pressure were applied sufficiently on the welds and heating intensively. In the molten zone boundaries, streamlines were observed in incompletely molten and sheared layers, which resulted from the combined effect of rapid cooling and shear stresses. Stereomicroscopy and SEM studies revealed the presence of unfused regions in the weld roots. SEM studies also revealed that compatibility of PP welds is higher than that of PVC welds.

Mechanical properties of welds exhibited good agreement with the results of calculated welding energy values as well as rheological studies [3]. The weld strengths of PE and PP sheets were higher than that of PVC for all welding procedures. These indicated that the weld strength increased with the increasing values of welding energy (E_w) as well as weldability (RW). The weld strength improved when the welding shoe was employed owing to the intensively heated weld region and application of sufficient welding pressure. Double V-welds with the welding shoe attained maximum weld strength although their second seams contained weakness.

Acknowledgements

The authors thank Dr. Feriha Ercan of Medical Faculty, Dr. Arif N. Güllüoğlu, Mustafa İlhan, and Özgür Çınar of Engineering Faculty, all of whom from Marmara University, for their helps during this work. Thanks also go to Ufuk Balkan, who is the youngest brother of the first author, for his assistance in developing photographs.

Nomenclature

c_p = Specific heat capacity of air (1.012 J g^{-1} K^{-1}).
E_w = Welding energy (kJ m^{-1}).
f_w = Weld factor (-).
F = Welding force (N).
P = Welding pressure (MPa).
q_v = Flow rate of the gas (38.33×10^{-4} m^3 s^{-1}).
S_w = Welding speed (mm s^{-1}).
t = Welding time (s).
T = Welding temperature (K).
$\dot{\varepsilon}$ = Strain rate (s^{-1}).
ε_y = Yield strain [%).
ρ = Density of air (1.2 kg m^{-3}).
σ_y = Yield stress (MPa).

References

[1] J. Abram, D.W. Clegg, D.V. Quayle, The strength of welds in uPVC, Plastics and Rubber International 7/2 (1982) 58-60.

[2] J.R. Atkinson, B.E. Turner, Repairability of plastic automobile bumpers by hot gas welding, Polymer Engineering Science 29/19 (1989) 1368-1375.

[3] O. Balkan, A. Ezdeşir, Rheological weldability of polymers, Proceedings of the 12th International Materials Symposium IMSP'2008, Denizli, 2008, in press.

[4] F. Becker, H. Potente, A step towards understanding the heating phase of laser transmission welding in polymers, Polymer Engineering and Science 42/2 (2002) 365-374.

[5] C. Bonten, E. Schmachtenberg, A new hypothesis to describe the mechanisms acting in a welded joint of semicrystalline thermoplastics, Polymer Engineering and Science 41/3 (2001) 475-483.

[6] J. Bowman, Butt fusion joining polyethylene pipes - and assessing the resultant joint strength, Welding and Metal Fabrication 64/2 (1996) 62-65.

[7] K. Cramer, Welded joints in thermoplastics, German Plastics 83/1 (1993) 9-10.

[8] G. Diedrich, B. Kempe, Welding of pipes and fitting made from different grades of HDPE, German Plastics 70/2 (1980) 14-15.

[9] M. Gehde, G.W. Ehrenstein, Structure and mechanical properties of optimized extrusion welds, Polymer Engineering and Science 31/7 (1991) 495-501.

[10] H. Gumbleton, Hot gas welding of thermoplastics – an introduction, Joining Materials 2/5 (1989) 215-218.

[11] G. Haim, Manual for Plastic Welding-III, Crosby Lockwood and Sons, London, 1959.

[12] S.L. Haller, U.S. Patent 3,839,126: Plastic welding apparatus, 1974.

[13] D. Hausdörfer, H. Herrmann, W. Muth, Multi-layer hot-gas welding of thick-walled rigid polyethylene mouldings, German Plastics 66/1 (1976) 4-6.

[14] J. Hessel, E. Mauer, The appearance of fractures in welded joints made of plastics following bending tests, Welding and Cutting 37/5 (1985) 76-77.

[15] P. John, J. Hessel, E. Gaube, A new development in the extrusion welding sector, German Plastics 75/1 (1985) 7-8.

[16] G.M. Kolbasuk, Hot wedge fusion welding of HDPE Geomembranes, Geotextiles and Geomembrans 9/4-6 (1990) 305-317.

[17] C.B. Lin, L.C. Wu, Friction welding of similar and dissimilar materials: PMMA and PVC, Polymer Engineering and Science 40/8 (2000) 1931-1941.

[18] T.T. Lin, S. Staicovici, A. Benatar, Non-contact hot plate welding of polypropylene Proceedings of the ANTEC Conference, 1996, 1260-1263.

[19] B. Marczis, T. Czigany, Polymer Joints, Perodica Polythechnica Ser. Mech. Eng. 46/2 (2002) 117-126.

[20] B. Marczis, T. Czigany, Interrelationships between welding parameters of hot-gas welded polypropylene, Polymer Engineering and Science 46/9 (2006) 1173-1181.

[21] B. Marczis, T. Czigany, Investigation of the heat affected zone of hot-gas welded PP joints, International Polymer Processing 21/2 (2006) 141-148.

[22] K.K. Mathur, S.B. Driscoll, Reduction of notch sensitivity and improvement in low-temperature impact strength of PVC, Journal of Vinyl Technology 4/2 (1982) 81-86.

[23] P. Michel, An analysis of the extrusion welding process, Proceedings of the ANTEC Conference, 1989, 482-487.

[24] P. Michel, An analysis of the extrusion welding process, Polymer Engineering and Science 29/13 (1989) 1376-1381.

[25] J.-Y. Nieh, L.J. Lee, Hot plate welding of polypropylene. Part I: Crystallization kinetics, Polymer Engineering and Science 38/7 (1998) 1121-1132.

[26] M.J. Oliveira, C.A. Bernardo, D.A. Hemsley, Morphology and mechanical behavior of polypropylene hot plate welds, Polymer Engineering and Science 41/11 (2001) 1913-1922.

[27] M.J. Oliveira, C.A. Bernardo, D.A. Hemsley, The effect of flame retardants on the hot-plate welding of talc-filled polypropylene, Polymer Engineering and Science 42/1 (2002) 146-151.

[28] H. Potente, J. Korte, R. Stutz, Laser-transmission welding of PE-HD, German Plastics 87/3 (1997) 27-29.

[29] R.C. Reinhardt, U.S. Patent 2,220,545: Method of welding thermoplastic materials, 1940.

[30] J. Rotheiser. Joining of Plastics: Handbook for Designers and Engineers, Carl Hanser Verlag, Munich, 1999.

[31] R.J. Sacks, Welding: Principles and Practices, Second Edition, Glencoe Division/McGraw-Hill, New York, 1981.

[32] E. Schmachtenberg, C. Tüchert, Long-term properties of butt-welded poly(propylene), Macromolecular Materials and Engineering 288/4 (2003) 291-300.

[33] M.M. Schwartz, Joining of Composite Matrix Materials, Chapter 2, ASM International, Ohio, 1994, 35-87.

[34] A. Shoh, Welding of thermoplastics by ultrasound, Ultrasonics 14/5 (1976) 209-217.

[35] J. Sims, P.A. Ellwood, H.J. Taylor, Pollutants from laser cutting and hot gas welding of plastics, Annals of Occupational Hygiene, 37/6 (1993) 665-672.

[36] V.K. Stokes, Joining methods for plastics and plastic composites: An overview, Polymer Engineering and Science 29/19 (1989) 1310-1324.

[37] S. Staicovici, C.-Y. Wu, A. Benatar, Z. Bahman, Fractal analysis and radiographic inspection of microwave welded HDPE bars, Proceedings of the ANTEC Conference, 1996, 1285-1289.

[38] V.K. Stokes, Hot-tool and vibration welding of poly(vinyl chloride), Journal of Vinyl and Additive Technology 6/3 (2000) 158-165.

[39] V.K. Stokes, Experiments on the induction welding of thermoplastics, Polymer Engineering and Science 43/9 (2003) 1523-1541.

[40] R.P. Wool, K.M. O'Connor, Time dependence of crack healing, Journal of Polymer Science, Polymer Letters Edition 20/1 (1982) 7-16.

[41] R.P. Wool, Molecular aspects of tack, Rubber Chemistry and Technology 57/2 (1984) 307-319.

[42] C.-Y. Wu, A. Benatar, , Single mode microwave welding of HDPE using conductive polyaniline/HDPE composites, Proceedings of the ANTEC Conference, 1995, 1244-1247.

[43] A. Yousefpour, M. Hojjati, L.-P. Immarigeon, Fusion bonding/welding of thermoplastic composites, Journal of Thermoplastic Composite Materials 17/4 (2004) 303-341.